Bollettino di Geofisica Teorica ed Applicata Vol. 59, n. 1, pp. 27-46; March 2018
DOI 10.4430/bgta0218

An investigation of local site effects in Adelaide, south Australia: learning from the past

B. Setiawan[1, 2], M. Jaksa[1], M. Griffith[1] and D. Love[3]

[1] *School of Civil, Environmental and Mining Engineering, the University of Adelaide, Australia*

[2] *Faculty of Engineering, Syiah Kuala University, Darussalam, Banda Aceh, Indonesia*

[3] *Department of State Development, the Government of South Australia, Adelaide, Australia*

(Received: June 20, 2017; accepted: December 20, 2017)

ABSTRACT Three major seismic events have damaged the Old Exchange Building, Adelaide, southern Australia. The building was graced by the Britannia statue on the parapet of the building. The statue lost its arm during the 1897 Beachport earthquake and bowed its helmeted head during the 1902 Warooka seismic event. It was removed after the 1954 Adelaide earthquake. Local site effects contributed significantly to the destruction of the Britannia statue. This paper investigates and presents the historical local site effects with respect to the Old Exchange Building. Synthetic ground motion time histories of the past three seismic events are generated and confirm the suitability of the method. Representative 1D soil profiles are developed and validated. Site response analysis was then carried out at the Old Exchange Building site to obtain the seismic parameters at the investigated site. The results are compared against historical intensity maps of the events, which are assumed as the actual spectral accelerations during the events. Hazard spectra and amplification triggered by the seismic events are deduced. This study reveals the significance of local site effects by an amplification factor of up to 3.4 that led to the destruction of the Britannia statue.

Key words: seismic, site effect, amplification, Adelaide, southern Australia.

1. Introduction

Of all Australia's cities, Adelaide is the most at risk of a severe earthquake (Standards Australia, 2007). In the last 150 years, the city has experienced more medium-sized earthquakes than any other Australian city. Three significant events include the 1897 Beachport earthquake, the 1902 Warooka earthquake, and the 1954 Adelaide earthquake (the 'three historical seismic events'), (McCue, 1990; Malpas, 1991; Dyster, 1996; Love, 1996). These three historical seismic events caused damage to the Old Exchange Building at Pirie St., Adelaide, southern Australia (Fig. 1). The damage was manifested in the Britannia statue located on the parapet of the building. The statue lost its arm during the 1897 Beachport earthquake [Modified Mercalli Intensity (MMI) IV-V], and its helmeted head was bent over in the 1902 Warooka seismic event (MMI V-VI). Due to heavy damage, the statue was finally removed after the 1954 Adelaide earthquake (MMI VI-VII) (Malpas, 1991; Dyster, 1996). Local site effects for the particular case of the Old Exchange Building have never been investigated.

Fig. 1 - The Old Exchange Building with the Britannia Statue on the parapet.

This study investigates the local site effects with respect to the Old Exchange Building, which is situated on a regolith site. The investigation is based on past seismic events.

Synthetic bedrock time histories of the three historic seismic events have been generated using EXSIM (Motazedian and Atkinson, 2005). The time histories are used in the 1D site response analyses to estimate the peak ground acceleration (PGA), and other seismic parameters (i.e. response spectral acceleration, velocity and displacement) at the Old Exchange Building site. The results are examined alongside the historical experiences and the intensity maps associated with the seismic events that are assumed the actual spectral accelerations during these events. The MMIs of the 1897 Beachport, 1902 Warooka, and 1954 Adelaide earthquakes were of IV-V, V-VI, and VI-VII, respectively (Malpas, 1991; Dyster, 1996). The comparison reveals the significance of local site effects in the damage manifested in the building. The findings from this study may form a basis for further comprehensive and systematic analyses of site effects and seismic-related studies in Adelaide, southern Australia.

2. The characteristics of the past seismic and geological setting of the investigated site (the Old Exchange Building site) and surrounding areas

As mentioned above, this study examines the impact of just three historical seismic events. These seismic events were estimated at 6.5, 6.0 and 5.3 on the Richter local magnitude scale (M_L) for the 1897 Beachport, 1902 Warooka and 1954 Adelaide earthquakes, respectively (Everingham *et al*., 1982). Both the 1897 Beachport and 1902 Warooka events caused extensive damage (MMI IX-VII) in the areas near the epicentre. These events were also felt at distances of hundreds of kilometres from the epicentres, including the city of Adelaide (Malpas, 1991). After about a half century, Kerr-Grant (1956) and McCue (1975) reported that Adelaide was shaken on March 1, 1954. This seismic event is the strongest earthquake in Adelaide's recorded history. Due to this

event, at least 30,000 insurance claims were made. Each of these three past seismic events testify to the need for estimating ground surface motion in the city, which includes site effects. The location of Adelaide, as well as the epicentres of the three major historical earthquakes (after Everingham *et al*., 1982), are shown in Fig. 2. The Old Exchange Building is located in the middle of the central business district (CBD) of Adelaide, as shown in Fig. 3.

The major geological structures of the Adelaide city and its surrounding region are fault segments that develop in a NE to SW direction. Most of the faults can be characterised by lithological disposition. There were several past seismic events associated with these faults as documented and presented by Selby (1984). The most significant event was associated with intra-plate activity along the Burnside-Eden Fault zone. This occurred on March 1, 1954, and is known as the 'Adelaide earthquake'. This seismic event was estimated at a magnitude of 5.3 (Selby, 1984; Love, 1996). Two main faults delimit the city of Adelaide to the west (Para Fault) and east (Eden-Burnside Fault). Both the Para and Eden-Burnside faults predominantly control the ground surface morphology of the city and its adjacent areas.

Most of the upper ground layer of Adelaide is made up of fill material and other surficial covers. Below the top fill and surficial cover, the subsurface profile is composed of Holocene deposits of Callabonna Clay and the Pooraka Formation. Beneath these Holocene deposits is the Hindmarsh Clay formation. Sheard and Bowman (1987a, 1987b) separated Keswick Clay from the Hindmarsh Clay formation below the Holocene deposits. Below these Quaternary deposits there is an unconformity beneath which are the Burnham Limestone and Hallett Cove Sandstone

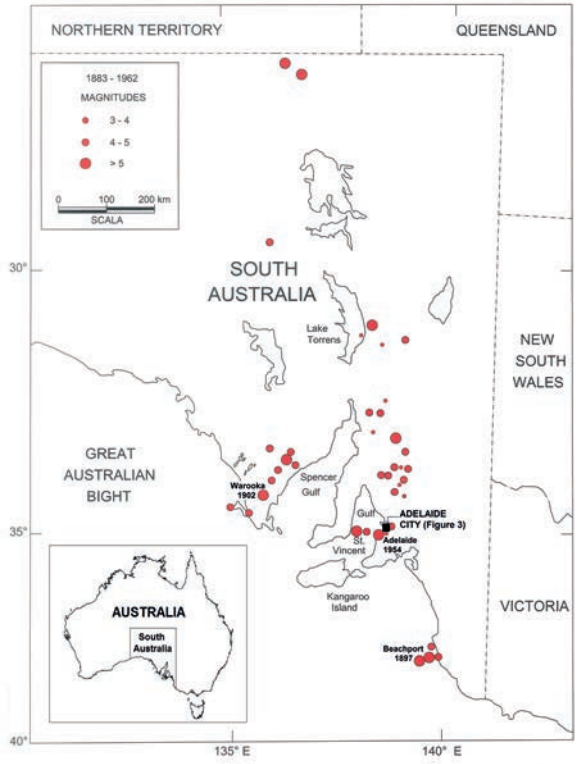

Fig. 2 - Locations of the epicentres of the South Australian historical seismic events, including the three events that damaged the Old Exchange Building (after Malpas, 1991).

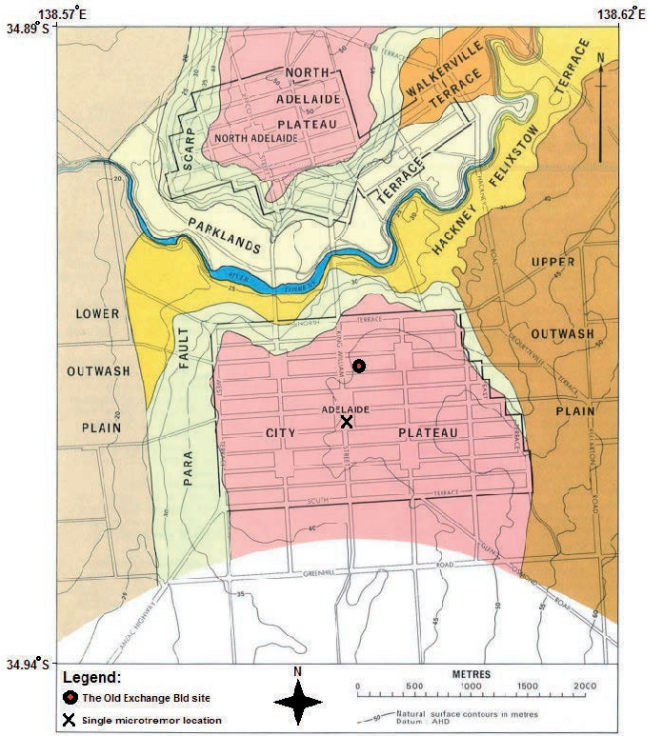

Fig. 3 - Morphology of the Adelaide city, with the location of the Old Exchange Building site.

Formation. Below this lies another unconformity followed by the sand unit of the Port Willunga Formation and the Tandanya Sand Member of the Chinaman Gully Formation. These units were deposited between the Pleistocene and Eocene (Selby and Lindsay, 1982). They are followed by the Undifferentiated Basal Blanche Point Formation and Tortachilla Limestone, South Maslin Sand and Clinton Formation, prior to the Precambrian bedrock. The reduced level of the bedrock is believed to be approximately 88.5 m or less to the north of the city, and can be up to 94.3 m or more below ground to the south of the city (Selby and Lindsay, 1982).

As shown in Fig. 3, much of the commercial development of the Adelaide city is founded on two morphological plateaus; one to the north and the other to the south of the city. The remaining morphologies, i.e. the upper outwash plain, lower outwash plain, terrace and fault scarps, are associated with either parklands or residential developments. Selby and Lindsay (1982) suggested that faults predominantly control the morphology of the city in the present day.

3. Methodology of this study

In this study, as there were no actual ground motions recorded for the three major historical seismic events, synthetic seismic motions are considered to represent the ground motions of these earthquakes. The generation of the synthetic seismic motions, as well as other parameters and site response analysis adopted in this study, are described below.

3.1. Generating input seismic motions

Table 1 details the main data associated with the seismic events of the 1987 Beachport, 1902 Warooka, and 1954 Adelaide earthquakes that were used to generate the seismic motions. This study uses a stochastic finite-fault model, EXSIM (Motazedian and Atkinson, 2005), to simulate the time histories of the 1897 Beachport, 1902 Warooka, and 1954 Adelaide earthquakes. There are some salient features of the adopted approach (EXSIM). Firstly, the model has been validated using a minimum of 300 strong motion stations at distances of 40 to 500 km (Motazedian and Atkinson, 2005; Atkinson and Macias, 2009). For the case of the close distance seismic event (i.e. 1954 Adelaide earthquake), an analytical model proposed by Mavroeidis and Papageorgiou (2003) is included in EXSIM. Secondly, the model was based on FINSIM (Beresnez and Atkinson, 1998) with ground motions generated by ruptures along faults. Thirdly, this finite-source model is appropriate for large earthquakes at relatively close distances (Hartzell, 1978; Joyner and Boore, 1986). Santulin *et al*. (2012) employed EXSIM for generating two historical earthquakes (the 1936 Cansiglio and 1976 Friuli earthquakes) in Italy. In the present study, additional parameters are needed to produce the synthetic ground motions as shown in Table 2. Most of the input parameters are adopted from Allen (2012). Additional parameters for analytical modelling proposed by Mavroeidis and Papageorgiou (2003) were employed in the case of the close distance seismic event. These additional parameters, shown in Table 2, have been validated by Motazedian and Moinfar (2006) against the 2003 Bam earthquake in SE Iran.

Four different input motions are considered. The first is a synthetic seismic motion generated for the 1897 Beachport event (earthquake of M_L 6.5 at a distance, R, of 260 km from the city of Adelaide). The second is a synthetic seismic motion produced for the 1902 Warooka event (earthquake of M_L 6.0 at R = 60 km from Adelaide). The third is a synthetic seismic motion calculated for the 1954 Adelaide event, considered the worst near-field seismic scenario for the city (earthquake of M_L 5.3 at R = 12 km from Adelaide). The fourth is a synthetic seismic motion calculated for the 1997 Burra event (earthquake of M_L 5.1 at R = 130 km from Adelaide). The first three synthetic ground motion time histories are shown in Fig. 4. These synthetic time histories are used for a site-specific ground response analysis of the site of interest, to estimate the PGA and validate site amplification during the 1897 Beachport, 1902 Warooka and 1954 Adelaide earthquakes. The fourth synthetic seismic motion for the 1997 Burra earthquake is generated to examine the suitability of the stochastic finite-fault model in this study. The application of this 1997 Burra synthetic seismic motion into the site response analysis of the investigated site is compared to the application of the actual recorded seismic motions at the Government House site (GHS) Adelaide, which is a similar model (Fig. 5). The GHS is a soil site and is located

Table 1 - Three historical seismic events contributed to the damage of the Old Exchange Building.

Event	Magnitude (M_L)	Depth (km)	Estimated distance (km)	Intensity at the investigated site	
				MMI	Reference
1897 Beachport earthquake	6.5	14	260	IV-V	McCue (1975)
1902 Warooka earthquake	6.0	4	60	V	McCue (1975)
				VI	Malpas (1991)
1954 Adelaide earthquake	5.3	4	12	VI-VII	After Malpas (1991)

Table 2 - Parameters for ground motion simulations using EXSIM (after Allen, 2012).

Input Parameter	Value	Remarks
Shear-wave velocity, β	3,600 m/s (Wesson, 1988)	Beta
Density, ρ	2,800 kg/m^3	Rho
Rupture propagation speed	0.8 β	Vrup
Brune stress drop, Δσ	23 MPa	Stress
Pulsing percentage	25%	Pulsing Percent
Geometrical attenuation R^b, b	–1.33 (0-90 km) +0.32 (90-150 km) –1.66 (> 150 km)	Gsprd
κ_0	0.006 s	Kappa
Distance-dependent duration	0.00 (0-10 km) +0.14 (10-70 km) –0.04 (70-160 km) +0.07 (> 160 km)	Trilinier duration and properties
Fault dip	35°	Dip
Earthquake magnitude (M)	6.5, 6.0 and 5.3	1898 Beachport, 1902 Warooka, and 1954 Adelaide earthquakes
Earthquake distance	260, 60 and 12 km	Distance from the epicentre of each earthquake to Adelaide CBD
Prevailing frequency ($f_P = 1/T_P$)	Log T_P = -2.2+0.4M	Parameters for the 1954 Adelaide earthquake only.
Phase angle	10°	
Oscillatory character	1.5	

approximately 0.5 km from the Old Exchange Building. A deconvolution of the generated time histories at bedrock level using EXSIM was carried out. This deconvolution of the time histories was compared to the actual time histories at the GHS site.

3.2. Developing a one-dimensional (1D) profile

Detailed knowledge of the subsurface characteristics of the investigated site contributed to generating a 1D profile for the investigated site. The subsurface lithology profiles of the investigated site are developed based on the work of Selby and Lindsay (1982). They examined an extensive amount of geotechnical borehole, groundwater and deep excavation data from which stratigraphic profiles and cross-sections of Adelaide were developed. Two boreholes (BH 42 and BH 83) were drilled by Selby and Lindsay (1982) near the Old Exchange Building site, and two sections (C-C and G-G) were developed by Selby and Lindsay (1982) from these boreholes.

From these two sections, two subsurface models are established in this study. The first model is based mainly on Section C-C, hereafter referred to as Model A. The second is established primarily from Section G-G, hereafter referred to as Model B. The total depth of both models A and B is up to the Pre-Cambrian bedrock. Both models A and B share similar geological formations from the ground surface down to the Pre-Cambrian bedrock. Slight differences in the thicknesses of the formations are observed due to the modest lateral heterogeneity of the geological formations.

In addition to the stratigraphic profile, in situ, ambient-noise single station and array measurements were conducted in order to quantify the shear wave velocity profiles in the Adelaide city (Setiawan *et al*., 2016).

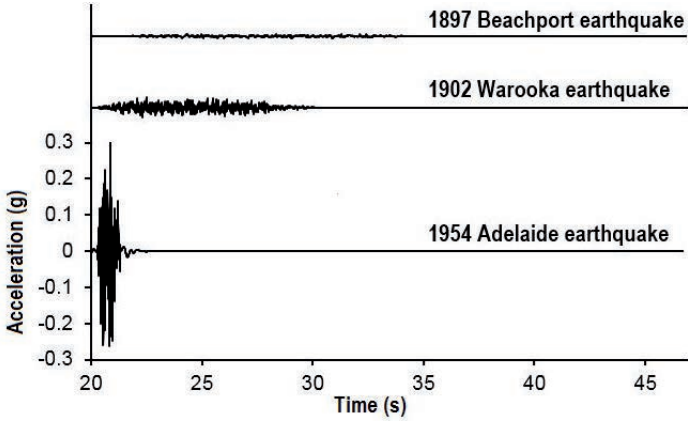

Fig. 4 - Synthetic acceleration time histories of the three past earthquakes.

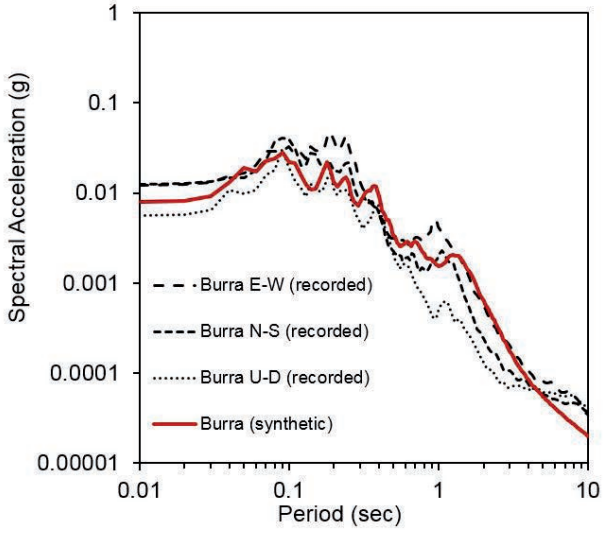

Fig. 5 - Response spectral acceleration validation of the synthetic time histories generated using the 1997 Burra seismic event.

A shear wave velocity profile at a location of approximately 200 m from the investigated site was developed by the authors (Setiawan *et al*., 2016). This shear wave velocity profile is incorporated into the 1D profile for the site response analysis at the investigated site. To validate the appropriateness of the shear wave velocity model deduced by Setiawan *et al*. (2016), a forward-computation of the model proposed by Garcia-Jerez *et al*. (2016) is employed to obtain a spectral ratio between the horizontal and vertical components (HVSR). The computed HVSR for the inverted 1D soil profiles is compared with the observed HVSR of the measured microtremor. The comparison of the mean HVSR observed by McCue and Love (1997), the mean HVSR observed by Setiawan *et al*. (2016), and the computed HVSR in this study, are presented in Fig. 6. Generally, the comparison between the observed and calculated HVSR curves show comparable results. Both the observed and calculated HVSRs suggest two-peak frequency characteristics at frequencies of about 0.8-0.9 and 4.0-5.0 Hz. The subsequent developed 1D profiles for the Old Exchange Building site are presented in Table 3.

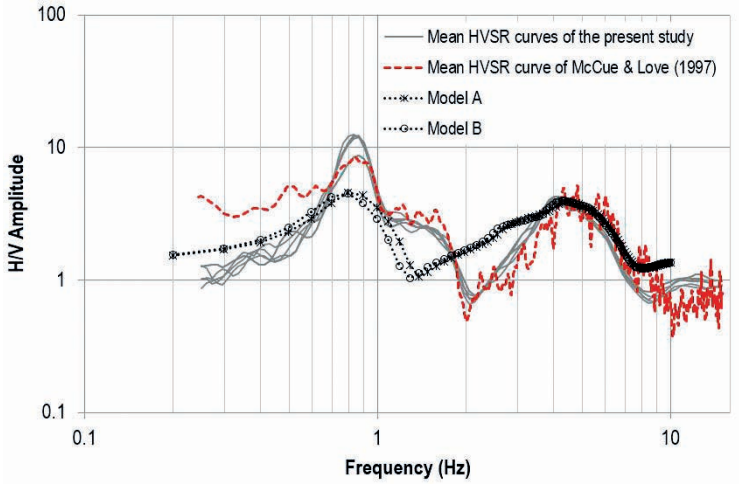

Fig. 6 - Comparison between the mean of the observed and calculated HVSR curves from the best fit models.

Table 3 - Developed 1D profiles for the investigated site.

Formation	Description	Thickness or (Depth)		Estimated mean shear wave (m/s)
		Model A	Model B	
Quaternary alluvium, Pooraka Formation [HOLOCENE]	Red brown silty CLAY (CH), grades downwards to SAND and GRAVEL (SP-GP)	2.4	2.3	137
Keswick CLAY [PLEISTOCENE]	Grey-green CLAY (CH) with red and brown mottling, stiff to hard, fissured	6.1	6.3	159
Hindmarsh CLAY [PLEISTOCENE]	Grey-green CLAY (CH) with yellow and red mottling with overlying SAND (SC)	6.1	6.3	354
Bunham Limestone and Hallett Cove Sandstone [PLEISTOCENE TO PLIOCENE]	White clayey, sandy and rubbly LIMESTONE; Pale grey to yellow brown calcareous SANDSTONE with layers of sand (SP)	7.9	9.1	433
Sand unit of Port Willunga Formation [EOCENE]	Fine silty SAND (SM)	5.5	4.0	330
Tandanya Sand Member of Chinaman Gully Formation [EOCENE]	Gravelly, clayey SAND (SC-GW)	9.7	12.6	333
Gull Rock Member of Blanche point Formation [EOCENE]	Alternating bands of cherty siltstone and grey SILT (ML)	21.8	22.9	317
Undifferentiated basal Blanche Point Formation and Tortachilla Limestone [EOCENE]	Green to dark grey clayey SAND (SC) with LIMESTONE	4.8	5.1	283
South Maslin Sand [EOCENE]	Dark grey, brown at depth, but weathering to red brown or yellow, silty SAND (SM) with pyrite lumps	10.3	11.4	261
Clinton Formation [EOCENE]	Dark grey CLAY (CL) with LIGNITE; irregular clayey SAND zones (SC)	13.9	14.3	269
Precambrian bedrock	White, pink, brown, purple, blue-grey and greenish grey with thin sandy bands, decomposed quartzite or quartz veins, high plasticity SILT slightly sandy, very stiff to hard with a moisture content well below the plastic limit > 480 kPa	(88.5)	(94.3)	926

3.3. Modulus reduction and damping curves

Ideally, for a site-specific ground response analysis, the modulus reduction and damping curves are developed in accordance with the samples obtained from the soil profile. However, as the default curves provided by SHAKE91 (Idriss and Sun, 1992) or EERA (Equivalent-linear Earthquake Response Analysis) (Bardet *et al.*, 2000) have proven to work well in most applications for site response analysis (Sykora and Davis, 1993; Uthayakumar and Naesgaard, 2004): this study has also adopted these curves (Fig. 7). Each curve represents a unique, typical

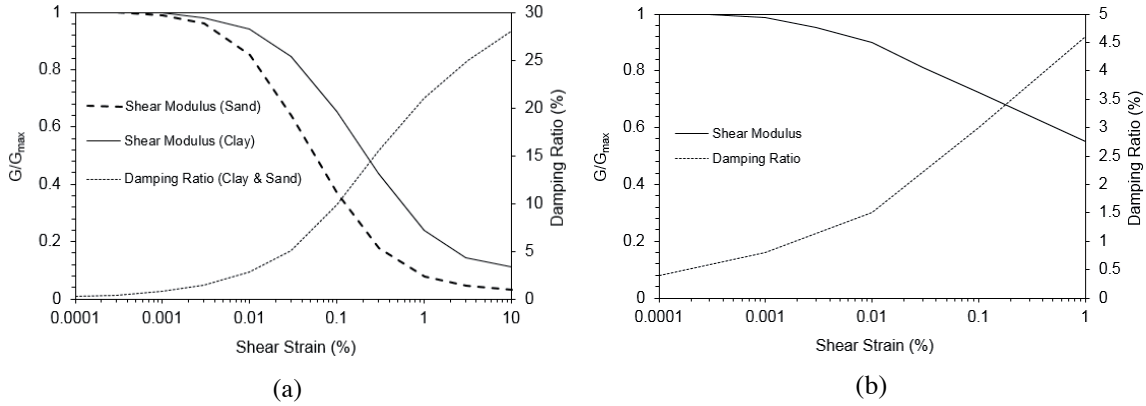

Fig. 7 - Shear modulus, shear strain and damping ratios for: a) clay (upper range) (Seed and Sun, 1989), sand (Seed and Idriss, 1970) and clay and sand damping ratio [Idriss (1990) cited by Bardet *et al.* (2000)], b) rock [Schnabel *et al.* (1972) cited by Bardet *et al.* (2000)].

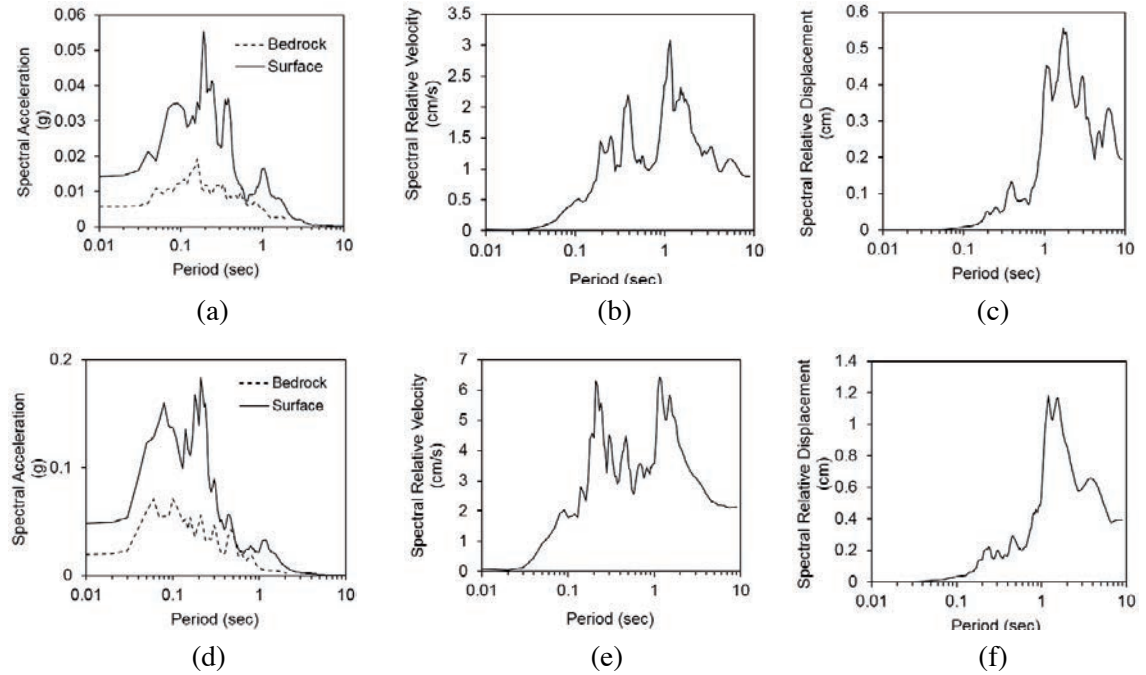

Fig. 8 - Model A input motion of 1897 Beachport earthquake: a) response spectral acceleration, b) velocity, and c) displacement outputs; and Model A input motion of 1902 Warooka earthquake: d) response spectral acceleration, e) velocity, and f) displacement outputs.

material behaviour during strain. The shear modulus reduction and damping ratio curves (Fig. 7a) were proposed by Seed and Sun (1989). The curves were developed from the upper bound shear modulus curve for clay (Seed and Sun, 1989). The shear modulus curve for sand (Fig. 7a) was by Seed and Idriss (1970). This was developed from the upper bound shear modulus curve of sand. The damping curves for clay and sand were proposed by Idriss (1990) cited by Bardet et al. (2000) (Fig. 7a), and for rocks by Schnabel *et al.* (1972) (Fig. 7b). In the present site response analysis, these curves are accordingly assigned to each layer of the subsurface model.

3.4. Conducting equivalent-linear site response analysis

Standard practice for the dynamic analysis of soils in geotechnical earthquake engineering is the equivalent-linear site response analysis (Borja *et al.*, 2000). This method assumes that soil stiffness and damping are consistent for a certain level of maximum shear-strain. It has been demonstrated that this analysis is able to reliably simulate soil behaviour due to dynamic loading (Priolo *et al*., 2008). This equivalent-linear site response analysis has been implemented in the SHAKE (Schnabel *et al*., 1972) computer program, which has been one of the most widely used tools for site response analysis for decades. The advantages of SHAKE are that it is simple and compact. Another equivalent-linear site response analysis program, EERA (Bardet *et al*., 2000), was developed by taking advantage of the most recent developments of FORTRAN 90 and the Windows operating system at the time. The EERA program was developed from the basic principles of SHAKE. Unlike SHAKE, EERA is an add-on program embedded in Microsoft Excel. Good agreement is obtained between the results of SHAKE and those of EERA for use in site-specific ground response analysis, as demonstrated by Bardet *et al*. (2000). As a result, EERA has been adopted here.

4. Results and discussions

Several outputs of the site-response analysis at the Old Exchange Building site, using the synthetic ground motions, are presented in Figs. 8a to 9c, for Model A, and in Figs. 9d to 10f, for Model B. The results are summarised in Tables 4 and 5 for Models A and B, respectively.

For Model A, the PGA results are 0.01, 0.06 and 0.30 g for the 1897 Beachport, 1902 Warooka and 1954 Adelaide seismic events, respectively. The estimated fundamental frequency of the site is estimated about 0.8 Hz. The response spectrum analysis, with a critical damping ratio of 5%, shows maximum spectral accelerations (SAs) for these events to be 0.06, 0.18 and 0.92 g for the 1987 Beachport, 1902 Warooka, and 1954 Adelaide earthquakes, respectively. The maximum spectral relative velocities (SVs) are estimated as equal to 3.1 cm/s for the 1897 Beachport event, 6.4 cm/s for 1902 Warooka event, and 36.8 cm/s for the 1954 Adelaide event. By considering the PGA, SA, and SV, the analysis here determines that the 1954 Adelaide earthquake presented the highest threat of all three to damage the Old Exchange Building. As expected, in terms of spectral displacement (SD), the highest displacement of the Old Exchange Building appears to have also resulted from the 1954 Adelaide earthquake. That earthquake generated a displacement of approximately 2.7 cm. The 1897 Beachport earthquake

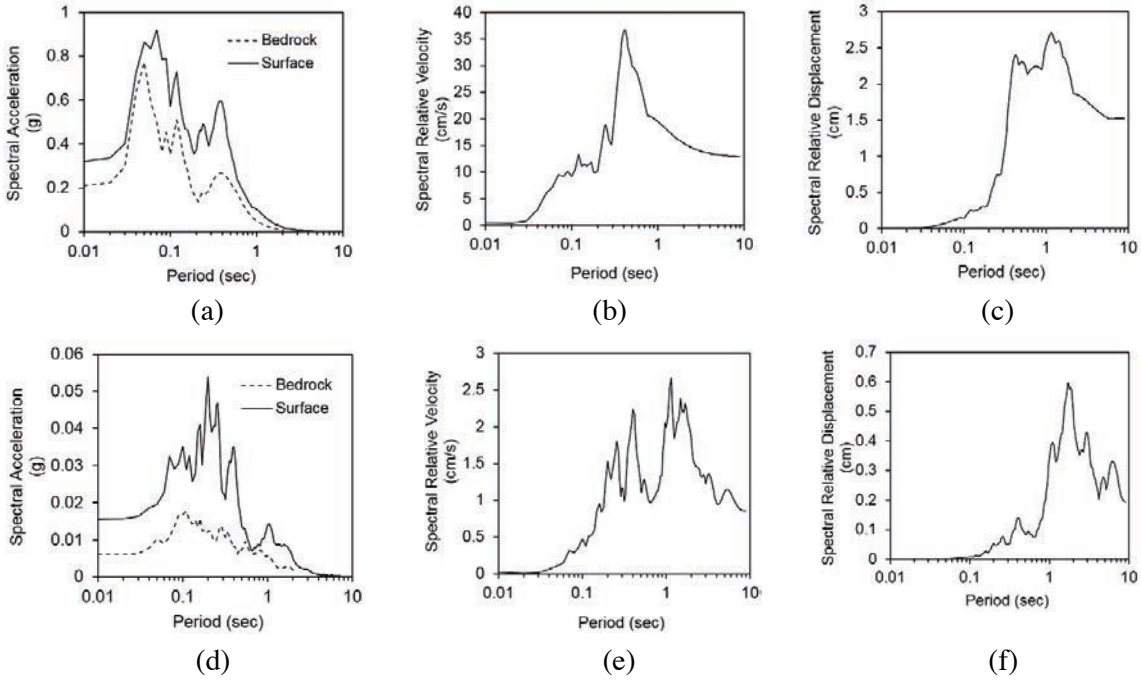

Fig. 9 - Model A input motion of 1954 Adelaide earthquake: a) response spectral acceleration, b) velocity, and c) displacement outputs; and Model B input motion of 1897 Beachport earthquake: d) response spectral acceleration, e) velocity, and f) displacement outputs.

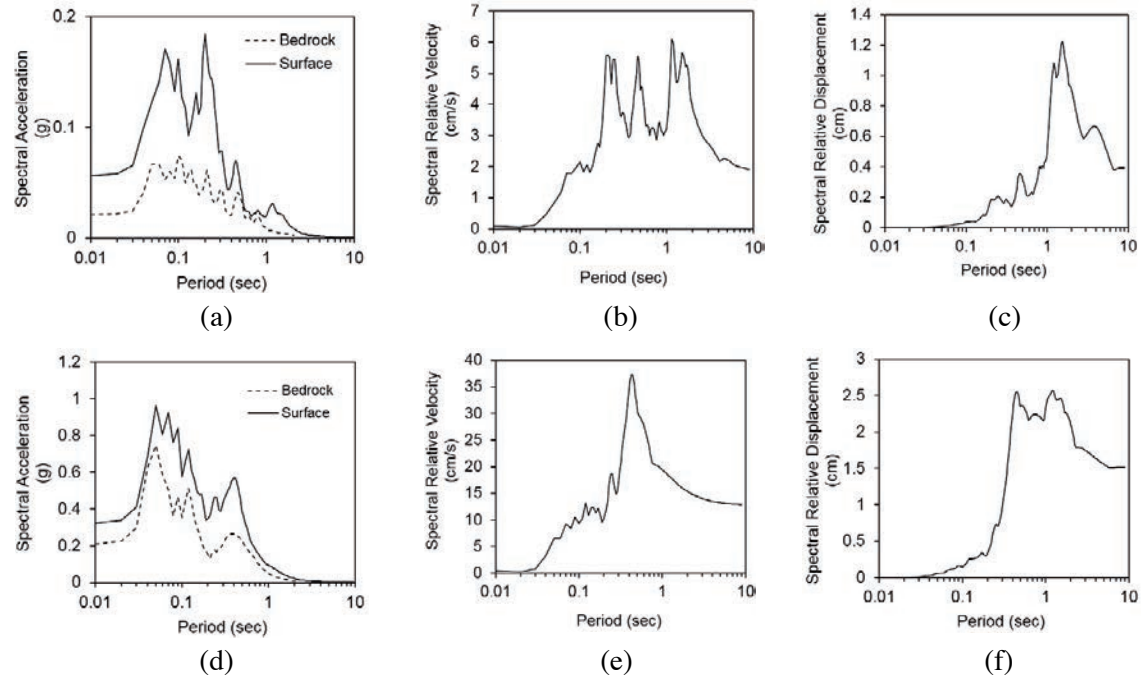

Fig. 10 - Model B input motion of 1902 Warooka earthquake: a) response spectral acceleration, b) velocity, and c) displacement outputs; and Model B input motion of 1954 Adelaide earthquake: d) response spectral acceleration, e) velocity, and f) displacement outputs.

Table 4 - Results of site-specific ground response analysis using EERA for Model A.

Parameters	1897 Beachport	1902 Warooka	1954 Adelaide
PGA (g)	0.014	0.049	0.321
Fundamental frequency (Hz)	0.800	0.800	0.800
Max spectral relative acceleration (g)	0.060	0.180	0.920
Max spectral relative velocity (cm/s)	3.080	6.430	36.800
Max spectral relative displacement (cm)	0.550	1.170	2.680

Table 5 - Results of site-specific ground response analysis using EERA for Model B.

Parameters	1897 Beachport	1902 Warooka	1954 Adelaide
PGA (g)	0.016	0.056	0.322
Fundamental frequency (Hz)	0.800	0.800	0.800
Max spectral relative acceleration (g)	0.050	0.180	0.960
Max spectral relative velocity (cm/s)	2.660	6.100	37.360
Max spectral relative displacement (cm)	0.580	1.210	2.560

caused a displacement of 0.55 cm, and the 1902 Warooka earthquake was estimated to cause a displacement of about 1.2 cm.

For Model B, the PGA results are 0.02, 0.06 and 0.32 g for the 1897 Beachport, 1902 Warooka, and 1954 Adelaide seismic events, respectively. Model B results in an estimated fundamental frequency at the Old Exchange Building site of 0.8 Hz. The maximum amplification for this model occurs at a frequency of 2.4 or 4.0 Hz. The response spectrum analysis, using a critical damping ratio of 5%, produces a maximum SA of 0.05, 0.18 and 0.96 g for the 1987 Beachport, 1902 Warooka, and 1954 Adelaide earthquakes, respectively. The maximum SV is 2.66 cm/s for the 1897 Beachport event, 6.1 cm/s for the 1902 Warooka event, and 37.4 cm/s for the 1954 Adelaide event. Among these three historical seismic events, Model B, again by considering the PGA, SA and SV, indicates that the 1954 Adelaide earthquake presented the highest threat of the three events. As with Model A, in terms of SD of the Old Exchange Building, the most critical value resulted from the 1954 Adelaide earthquake. This event again produced a displacement approximately 2.6 cm. The 1897 Beachport and 1902 Warooka earthquakes are estimated to cause displacements of approximately 0.58 and 1.20 cm, respectively.

The use of the analytical approach by Mavroeidis and Papageorgiou (2003) in the generation of the near source seismic event (i.e. Adelaide earthquake) in this study has several consequences on the results of the site response analysis. It estimates the PGA of up to 0.3 g, which generally provides better estimation than without the Mavroeidis and Papageorgiou (2003) analytical approach. This 0.3 g PGA for the 1954 Adelaide seismic event slightly overestimates the actual damage for this MMI of VI-VII event (see the later discussion). Furthermore, the analytical approach by Mavroeidis and Papageorgiou (2003) in the Adelaide earthquake case allows EXSIM to generate the long-period velocity pulses (Motazedian and Atkinson, 2005). This extension will

simulate low frequency or long period ground motion components. An amplification of the long period of the ground motion coherent components (i.e. velocity and displacement) is unavoidable in such near-source seismic events (Mimoglou *et al.*, 2017). The application of the analytical approach by Mavroeidis and Papageorgiou (2003) has increased the maximum SV up to 36.8 cm/s in Model A and up to 37.4 cm/s in Model B. The maximum spectral displacement of the Adelaide earthquake has also increased up to 2.7 cm in Model A and up to 2.6 cm in Model B. By contrast, the site response analyses without the application of the Mavroeidis and Papageorgiou (2003) analytical approach suggest the maximum spectral velocity of 20.9 cm/s for Model A, 23.4 cm/s for Model B and the maximum SD of 0.9 cm for both Models A and B (not shown in this paper). The effect of the seismic duration on the velocity component of ground motion was also suggested by Tehranizadeh and Hamedi (2000). The SV and displacement amplification on the inelastic response of structures due to near seismic sources is also reported by Panagiotou (2008), Iervolino and Cornell (2008), and Taflampas and Psycharis (2008). Therefore, the site response analysis results of the spectral relative velocity and displacement of the Adelaide earthquake must be carefully examined.

The PGA outputs from our study are compared with the empirical attenuation function by Wald *et al*. (1999) and Linkimer (2008), as shown in Table 6. The PGA calculations, using the empirical attenuation functions, are based on the seismic MMIs of IV-V, V-VI, and VI-VII for the 1897 Beachport, 1902 Warooka, and 1954 Adelaide earthquakes, respectively. The comparison suggests good agreement with the results of both the 1897 Beachport and 1902 Warooka earthquakes. However, this study suggests a slightly higher seismic intensity resulting from the 1954 Adelaide earthquake.

5. Hazard spectra

Log-log plots of the spectral accelerations for both Models A and B for the three historical seismic events are shown in Fig. 11. As mentioned above, the 1954 Adelaide earthquake is estimated to result in higher spectral accelerations than others, particularly below a period of 0.4 s.

Seismic event	Estimated MMI at Old Exchange Building site	Estimated PGA (g)		
		Wald *et al*. (1999)	Linkimer (2008)	Present study
1897 Beachport	IV-V (McCue, 1975; Dyster, 1996)	0.020 to 0.070	0.020 to 0.060	0.014 to 0.016
1902 Warooka	V-VI (McCue, 1975; Malpas, 1991)	0.070 to 0.130	0.060 to 0.110	0.049 to 0.056
1954 Adelaide	VI-VII (Malpas, 1991)	0.130 to 0.240	0.110 to 0.200	0.320

Table 6 - Comparison PGA estimation at the Old Exchange Building site.

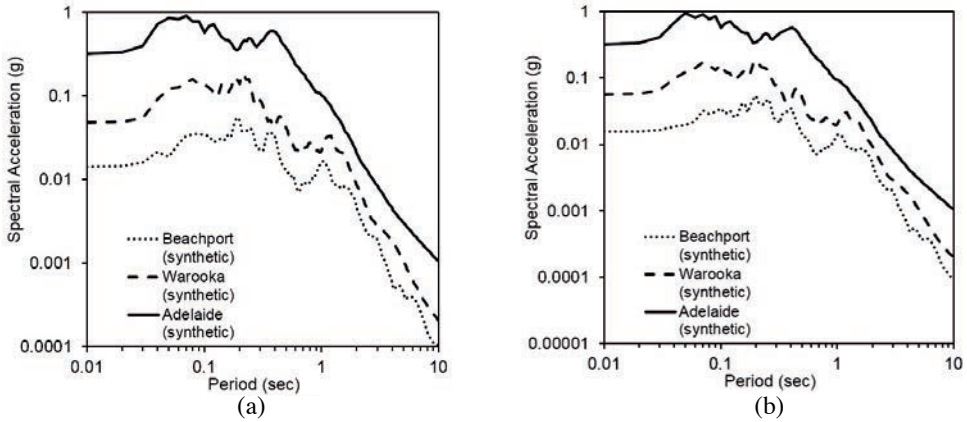

Fig. 11 - Response spectral accelerations of site response analysis for: a) Model A; b) Model B.

The spectral acceleration outputs are compared with the results of Love (1996) and Leonard *et al*. (2013). The maximum SA obtained is 0.92 g, which is associated with the 1954 Adelaide earthquake. Love (1996) suggested a maximum SA of 0.76 g and Leonard *et al*. (2013) estimated a value of approximately 0.30 g for a 2,500-year return period. Hence, our study has obtained slightly larger estimated SAs than those proposed by Love (1996). Furthermore, this work suggests a maximum SA three times larger than that suggested by Leonard *et al.* (2013). This large discrepancy is likely to be caused by the adopted shear wave velocity profile, modulus reduction and damping curves, and input ground motion. Our study adopts shear wave velocity profiles based on forward modelling of the measured HVSR curves with an average of the top 30 m shear wave velocity (V_{s30}) between 315 and 320 m/s, whereas Leonard *et al.* (2013) most likely employed an empirical shear wave profile with V_{s30} between 315 and 460 m/s. The study here employs the generic modulus reduction and damping curves, whereas Leonard *et al.* (2013) likely used different modulus reduction and damping curves. In terms of input ground motions, we selected the ground motions based on past seismic events (i.e. 1897 Beachport, 1902 Warooka, and 1954 Adelaide earthquakes), whereas the seismic event adopted by Leonard *et al.* (2013) is based on a probabilistic analysis. The paucity of strong motion events in the low-moderate seismic region of southern Australia, influences the results of such probabilistic analysis, as the seismic source zone is difficult to define.

6. Site amplification

Site amplification can be estimated using a comparison between the maximum acceleration of the ground surface layer and the maximum acceleration at bedrock level. Site response analysis results of the maximum acceleration profile at the Old Exchange Building site for models A and B are shown in Figs. 12a and 12b. These maximum acceleration profiles are used to deduce the amplification factor at the investigated site. The results are shown in Figs. 12c and 12d, which indicate an amplification factor at the ground surface level for Model A of between 1.5 to 2.5 and Model B of 1.5 to 2.6.

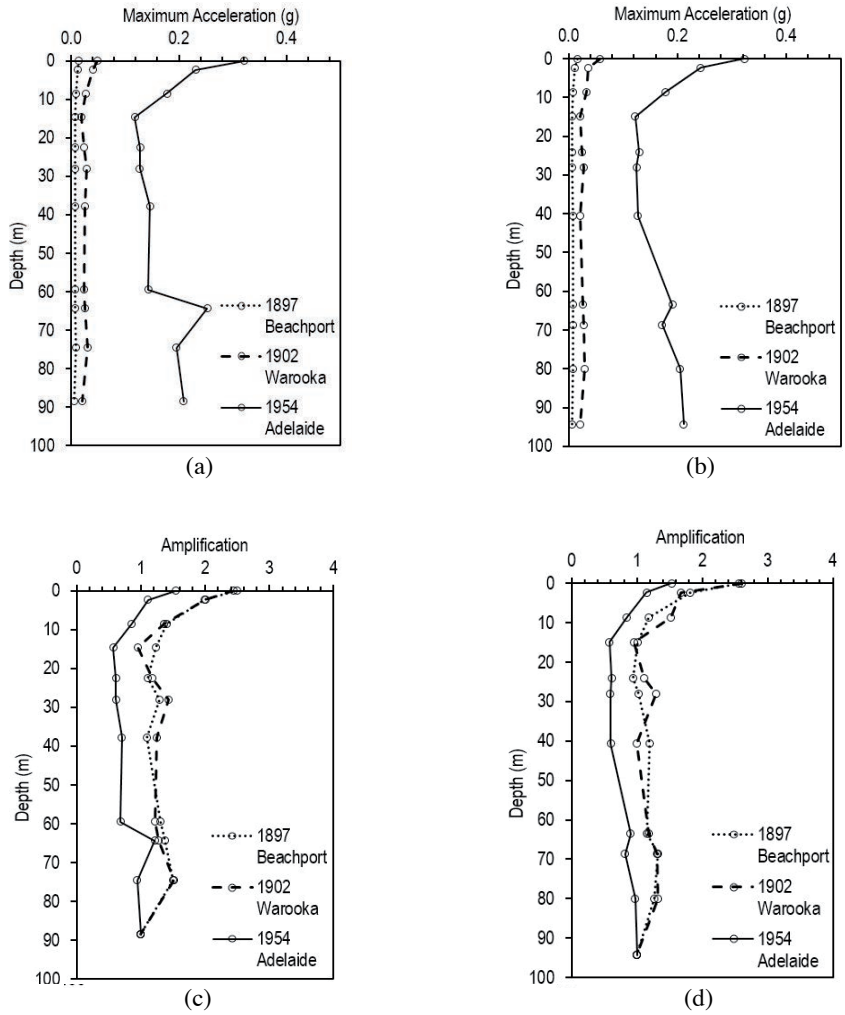

Fig. 12 - Site response analysis results: maximum acceleration profiles for Model A (a), and Model B (b), and amplification profiles for Model A (c) and Model B (d).

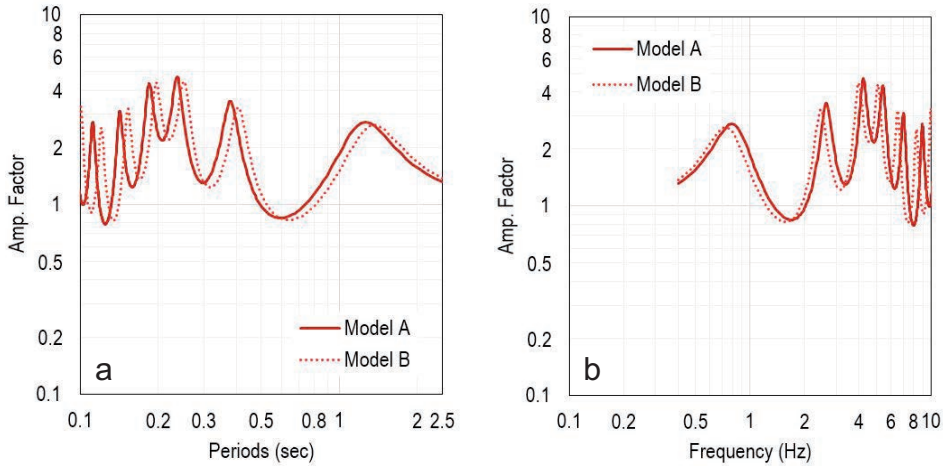

Fig. 13 - Amplification factors plotted against period (a) and frequency (b) at the Old Exchange Building site.

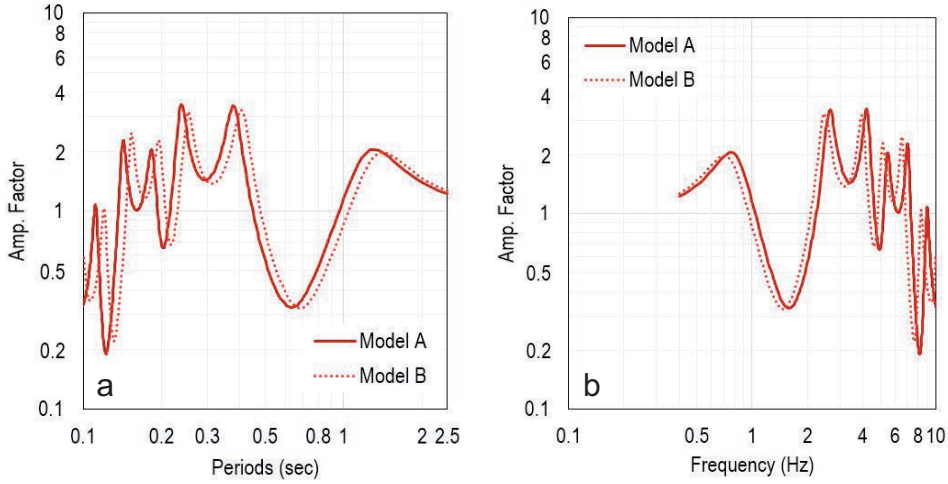

Fig. 14 - DAFs plotted against period (a) and frequency (b) at the Old Exchange Building site.

Site amplification factors are used to understand the seismic motion behavior in the study area by means of the method proposed by Herak (2008), which has been shown to yield reliable results (Herak *et al.*, 2010; Lunedei and Albarello, 2015). The mean compression wave, shear wave and density models obtained here are used to quantify the amplification factors. The quality factors of Q_p and Q_s, for the compression and shear waves, respectively, are estimated using the approaches suggested by Olsen *et al*. (2003) and Zhang and Stewart (2007), respectively, which represent a linear estimate of amplification.

The results of the site amplification factors (Amp-HVSR) are presented in Fig. 13. Generally, a site amplification of up to 3.4 is suggested. Averaging the amplification from 0.4 to 10 Hz at each site implies that the amplification factor is only 1.2. By using identical subsurface models, a dynamic amplification factor (DAF) for the investigated site is also calculated. The method proposed by Herak (2008) is employed to calculate DAF. Unlike the Amp-HVSR, the DAF uses the most likely seismic event in the calculation. Generally, the result of this study shows that the estimated DAF slightly overestimates the amplification analysis using the Amp-HVSR method. As shown in Fig. 14, the obtained value of DAF is 1.9.

As stated by Herak (2008), the amplification factors of both Amp-HVSR and DAF do not consider the non-linear behavior of the subsurface material. Therefore, these estimates need to be judiciously applied in practice. Whilst a non-linear site response analysis could potentially yield more reliable estimates, this is beyond the scope of the work here.

Additional evidence of site amplification in Adelaide is obtained from the recorded ground motions that occurred during the 1997 Burra earthquake. The recorded earthquake ground accelerations in Adelaide's regolith have been shown to be very much stronger than those recorded on bedrock just outside the city during this seismic event (DMITRE Minerals, 2013). Ground response analyses using historical ground motions also confirm site amplification. Thus, site amplification contributed to the damage experienced by the Old Exchange Building, as has been demonstrated to occur to similar buildings, such as in Mexico (Booth *et al*., 1986; Finn and Wightman, 2003), Kobe (Brebbia, 1996), and Umbria-Marche-Italy (Bindi *et al*., 2004; Castro *et al*., 2004; Luzi *et al*., 2005).

7. Site fundamental frequency

For the Old Exchange Building site, observed HVSR curves by McCue and Love (1997) and Setiawan *et al*. (2016), have indicated a site fundamental frequency of 0.7-0.8 Hz (as shown in Fig. 6) and first mode frequency of 4.0-4.5 Hz. Good agreement between both the observed HVSR curves of McCue and Love (1997) and Setiawan *et al*. (2016) highlight the consistency of the HVSR method with respect to time, as the measurement of the first reference was carried out in 1997, whereas the HVSR data of the later reference were obtained in 2015. This temporal stability of the HVSR analysis was also suggested by Okada (2003). The obtained site frequencies are also correlated to the Old Exchange Building frequency to analyze the possibility of resonance effects which will occur when the ground frequency is equal or close to the natural frequency of the building. In terms of the number of stories (N), the Old Exchange Building was a low-rise (3 story) building. By adopting the building fundamental frequency approximation of Kramer (1996), which is approximated by 10/N (Hz), the Old Exchange Building frequency is estimated to be between 3.0 and 3.5 Hz. As mentioned above, the observed site fundamental frequency at the Old Exchange Building site is 0.8-0.9 Hz, which is three times lower than the Old Exchange Building's natural frequency. However, the first mode site frequency (4.0-4.5 Hz) is relatively close to the Old Exchange Building's natural frequency. This implies that the first mode of site frequency is likely to have increased the Old Exchange Building's vibration and enhanced the prospect of structural collapse.

8. Study limitations and future work

While this study has provided useful information relating to site effects, the analysis is limited. Firstly, the study is confined to a specific case at a single site (i.e. the Old Exchange Building case). Clearly, extending the study to incorporate several sites across the city of Adelaide is desirable to obtain a more reliable prediction of the dynamic characteristics of Adelaide's sub-surface. However, given the limited data currently available, such additional analyses are not possible at this time. Secondly, the sub-surface shear wave velocity models were developed from forward modelling of a measurement obtained at a distance of approximately 200 m from the site. Again, it is preferable for the direct shear wave velocity measurement to be obtained at the site of interest. However, this was not possible due to access constraints. Finally, soil-structure interaction effects were not considered here and are beyond the scope of this study. Future improvements include extending the use of ambient vibration measurements for site characterisation in regolith environments and enhancing geophysical methods to investigate the basin structure of the investigated site.

9. Conclusion

Three historical seismic events, the 1897 Beachport (MMI IV-V), 1902 Warooka (MMI V-VI), 1954 Adelaide (MMI VI-VII) earthquakes, caused damage to the Old Exchange Building located

in Pirie St., Adelaide. As there were no recorded time histories of the three events, generated time histories are required. Time histories of the three events have been generated using a method that was validated using recorded ground motions of the 1997 Burra earthquake. Two representative models for the Old Exchange Building site were developed and validated using a single microtremor measurement at the nearby site.

The results of both the synthetic time histories of historical seismic events and the development of 1D profiles of the Old Exchange Building site, were used for investigating site effects. Analytical models used in this study for a site-specific ground response analysis proved to simulate the ground behaviour reasonably well. The results of the ground response analyses clearly indicate that, for the case of Old Exchange Building site, the input parameters are influenced by local site effects by an amplification factor of up to 3.4.

Acknowledgments. The authors wish to acknowledge the University of Adelaide for providing a research scholarship for the first author. In addition, the first author is grateful to the Faculty of Engineering of Syiah Kuala University for their support. The authors also acknowledge the editorial assistance of Leticia Mooney.

REFERENCES

Allen T.I.; 2012: *Stochastic ground-motion prediction equations for southeastern Australian earthquakes using updated source and attenuation parameters*. Geosci. Australia, Canberra, Australia, Record 2012/69, 76 pp.

Atkinson G.M. and Macias M.; 2009: *Predicted ground motions for great interface earthquakes in the Cascadia subduction zone.* Bull. Seismol. Soc. Am., **99**, 1552-1578, doi:10.1785/0120080147.

Bardet J.P., Ichii K. and Lin C.H.; 2000: *EERA a computer program for equivalent-linear earthquake site response analyses of layered soil deposits*. Dept. of Civil Eng., Univ. of Southern California, Los Angeles, CA, USA, 38 pp.

Beresnev I.A. and Atkinson G.M.; 1998: *FINSIM-a FORTRAN program for simulating stochastic acceleration time histories from finite faults*. Seismol. Res. Lett., **69**, 27-32.

Bindi D., Castro R.R., Franceschina G., Luzi L. and Pacor F.; 2004: *The 1997-1998 Umbria- Marche sequence (central Italy): source, path and site effects estimated from strong motion data recorded in the epicentral area*. J. Geophys. Res., **109**, B04312, doi:10.1029/2003JB002857.

Booth E.D., Pappin J.W., Mills J.H., Degg M.R. and Steedman R.S.; 1986: *The Mexican earthquake of 19th September 1985*. Earthquake Eng. Field Invest. Team (EEFIT), Soc. Earthquakes Civ. Eng. Dyn., London, U.K., 146 pp.

Borja R.I., Lin C-H., Sama K.M. and Masada G.M.; 2000: *Modelling non-linear ground response of non-liquefiable soils*. Earthquake Eng. Struct. Dyn., **29**, 63-83.

Brebbia C.A. (ed); 1996: *The Kobe earthquake: geodynamical aspects*. Comput. Mech. Publ., Southampton, U.K., 145 pp.

Castro R.R., Pacor F., Bindi D., Franceschina G. and Luzi L.; 2004: *Site response of strong motion stations in the Umbria region, central Italy*. Bull. Seismol. Soc. Am., **94**, 576-590.

DMITRE Minerals (Department of Manufacturing, Innovation, Trade, Resources and Energy Official Website); 2013: *Urban monitoring*. <www.pir.sa.gov.au/minerals/earthquakes/urban_monitoring accessed on 2 November 2013>.

Dyster T.; 1996: *Strong shock of earthquake: the strong of the four greatest earthquakes in the history of South Australia*. Dept. Mines and Energy, Geol. Surv. South Australia, Report Book 95/47.

Everingham I.B., McEwin A.J. and Denham D.; 1982: *Atlas of isoseismal maps of Australian earthquakes*. Dept. National Dev. & Energ., Bur. of Min. Resour., Geol. and Geophys., Canberra, Australia, Bull. 214, 184 pp.

Finn W.D.L. and Wightman A.; 2003: *Ground motion amplification factors for the proposed 2005 edition of the national building code of Canada*. Can. J. Civ. Eng., **30**, 272-278, doi:10.1139/l02-081.

García-Jerez A., Piña-Flores J., Sánchez-Sesma F.J., Luzón F. and Perton M.; 2016: *A computer code for forward computation and inversion of the HVSR spectral ratio under the diffuse field assumption.* Comput. Geosci., **97**, 67-78.

Hartzell S.; 1978: *Earthquake aftershocks as Green's functions.* Geophys. Res. Lett., **5**, 1-14.

Herak M.; 2008: *ModelHVSR-a Matlab tool to model horizontal-to-vertical spectral ratio of ambient noise*. Comput. Geosci., **34**, 1514-1526, doi:10.16/j.cageo.2007.07.009.

Herak M., Allegretti I., Herak D., Kuk K., Kuk V., Maric K., Markusic S. and Stipcevic J.; 2010: *HVSR of ambient noise in Ston (Croatia): comparison with theoretical spectra and with the damage distribution after the 1996 Ston-Slano earthquake*. Bull. Earthquake Eng., **8**, 483-499.

Idriss I.M.; 1990: *Response of soft soil sites during earthquakes*. In: Proc. H. Bolton Seed Memorial Symposium, Duncan J.M. (ed), BiTech Publishers, Vancouver, BC, Canada, pp. 273-289.

Idriss I.M. and Sun J.I.; 1992: *User's manual for SHAKE91 (a computer program for conducting equivalent linear seismic response analyses of horizontally layered soil deposits*. Centre Geotech. Model., Dept. Civ. and Environ. Eng., Univ. of California, Davis, CA, USA, 12 pp.

Iervolino I. and Cornell C.A.; 2008: *Probability of occurrence of velocity pulses in near-source ground motions*. Bull. Seismol. Soc. Am., **98**, 2262-2277.

Joyner W. and Boore D.; 1986: *On simulating large earthquakes by Green's-function addition of smaller earthquakes*. In: Proc. 5th Maurice Ewing Symp. Earthquake Source Mech., S. Das, J. Boatwright and C. Scholz (eds), Am. Geophys. Union, Washington, DC, USA, pp. 269-274.

Kerr-Grant C.; 1956: *The Adelaide earthquake of 1st March 1954*. Trans. Royal Soc. South Australia, **59**, 177-185.

Kramer S.L.; 1996: *Geotechnical earthquake engineering*. Prentice Hall, Upper Saddle River, NJ, USA, 673 pp.

Leonard M., Burbidge D. and Edwards M.; 2013: *Atlas of seismic hazard maps of Australia: seismic hazard maps, hazard curves and hazard spectra*. Geosci. Australia, Canberra, Australia, Record 2013/41, 39 pp.

Linkimer L.; 2008: *Relationship between peak ground acceleration and modified Mercalli intensity in Costa Rica.* Rev. Geol. America Central, **38**, 81-94.

Love D.; 1996: *Seismic hazard and microzonation of the Adelaide metropolitan area*. Sutton Earthquake Centre, Dept. of Mines and Energy South Australia, Adelaide, Australia, Report 27, 104 pp.

Lunedei E. and Albarello D.; 2015: *Horizontal-to-vertical spectral ratios from a full-wavefield model of ambient vibrations generated by a distribution of spatially correlated surface sources*. Geophys. J. Int., **201**, 1140-1153.

Luzi L., Bindi D., Franceschina G., Pacor F. and Castro R.; 2005: *Geotechnical site characterisation in the Umbria Marche area and evaluation of earthquake site-response*. Pure Appl. Geophys., **162**, 2133-2161, doi:10.1007/s00024-005-2707-6.

Malpas K.L.; 1991: *Seismic risk of South Australia*. Master Thesis, School of Earth Sci., Flinders Univ., Adelaide, South Australia, 179 pp.

Mavroeidis G.P. and Papageorgiou A.S.; 2003: *A mathematical representation of near-fault ground motions*. Bull. Seismol. Soc. Am., **93**, 1099-1131.

McCue K.; 1975: *Seismicity and seismic risk in South Australia*. Dept. of Phys., Univ. of Adelaide, South Australia, Report ADP 137.

McCue K.; 1990: *Australia's large earthquakes and recent fault scarps*. J. Struct. Geol., **12**, 761-766.

McCue K. and Love D.; 1997: *Earthquake microzonation Adelaide, South Australia*. Australian Geol. Surv. Organ. (AGSO), Final Report, 22 pp.

Mimoglou P., Psycharis I.N. and Taflampas I.; 2017: *Determination of the parameters of the directivity pulse embedded in near-fault ground motions and its effect on structural response*, In: Papadrakakis M., Plevris V. and Lagaros N.D. (eds), Computational methods in earthquake engineering, Springer, DOI:10.1007/978-3-319-47798-5_2.

Motazedian D. and Atkinson G.M.; 2005: *Stochastic finite fault modeling based on a dynamic corner frequency*. Bull. Seismol. Soc. Am., **95**, 995-1010.

Motazedian D. and Moinfar A.; 2006: *Hybrid stochastic finite fault modeling of 2003, M6.5, Bam earthquake (Iran)*. J. Seismol., **10**, 91-103, doi:10.1007/s10950-005-9003-x.

Okada H.; 2003: *The microtremor survey method*. Soc. of Explor. Geophys., Geophys. Monogr. Ser. No. 12, 150 pp., doi:10.1190/1.9781560801740, (Translated by Koya Suto).

Olsen K.B., Day S.M. and Bradley C.R.; 2003: *Estimation of Q for Long-Period (>2 sec) waves in the Los Angeles Basin*. Bull. Seismol. Soc. Am., **93**, 627-638.

Panagiotou M.; 2008: *Seismic design, testing and analysis of reinforced concrete wall buildings*. Ph.D. Dissertation in Struct. Eng., Univ. of California, San Diego, CA, USA, 289 pp.

Priolo E., Poli M.E., Laurenzano G., Vuan A. and Barnaba C.; 2008: *Site response estimation in the Vittorio Veneto area (NE Italy), Part 2: mapping the local seismic effects in the urban settlement*. Boll. Geof. Teor. Appl., **49**, 387-400.

Santulin M., Moratto L., Sarao A. and Slejko D.; 2012: *Ground motion modelling including finite fault and 1D site effects in north-eastern Italy*. Boll. Geof. Teor. Appl., **53**, 313-330, doi:10.4430/bgta0071.

Schnabel P.B., Lysmer J. and Seed H.B.; 1972: *SHAKE: A computer program for earthquake response analysis of horizontally layered sites*. Report 72-12, Earthquake Engineering Research Center, University of California, Berkeley, California, 102 pp.

Seed H.B. and Idriss I.M.; 1970: *Soil moduli and damping factors for dynamic response analysis*. Report No. UCB/EERC-70/10, Earthquake Engineering Research Center, University of California, Berkeley, California, 48 pp.

Seed H.B. and Sun J.H.; 1989: *Implication of site effects in the Mexico City earthquake of September 19, 1985 for earthquake-resistance-design criteria in the San Francisco Bay Area of California*. Report No. UCB/EERC-89/03, Earthquake Engineering Research Center, University of California, Berkeley, California, 140 pp.

Selby J.; 1984: *Geology and the Adelaide environment*. South Australian Dept. of Mines and Energy, Adelaide, Australia, 168 pp.

Selby J. and Lindsay J.M.; 1982: *Engineering geology of the Adelaide city area*. Dept. of Mines and Energy, Geol. Surv. of South Australia, 91 pp.

Setiawan B., Jaksa M., Griffith M. and Love D.; 2016: *Analysis of microtremor array measurement using the spatial autocorrelation (SPAC) method across the Adelaide city*. School of Civil, Environ. and Mining Eng., Univ. of Adelaide, Australia, Research Report No. R196, 36 pp.

Sheard M.J. and Bowman G.M.; 1987a: *Definition of the Keswick Clay: Adelaide/Golden Grove embayment, para and eden blocks, South Australia*. Quarterly Geol. Notes of the Geol. Surv. of South Australia, **103**, 4-8.

Sheard M.J. and Bowman G.M.; 1987b: *Redefinition of the upper boundary of the Hindmarsh Clay: Adelaide Plains Sub-Basin and Adelaide/Golden Grove embayment*. Quarterly Geol. Notes of the Geol. Surv. of South Australia, **103**, 9-16.

Standards Australia; 2007: *AS 1170.4-2007 Australian standard of structural design actions Part 4: earthquake actions in Australia.* Standards, Australia, 48 pp., <www.standards.org.au>.

Sykora D.W. and Davis J.J.; 1993: *Site-specific earthquake response analysis for Paducah gaseous diffusion plant, Paducah, Kentucky*. U.S. Dept. of Energy, Vicksburg, MS, USA, 266 pp.

Taflampas I. and Psycharis I.N.; 2008: *Investigation of the effect of the ground motion characteristics on the Ry-l relation for the inelastic response of SDOF structures*. In: Proc. 14th World Conf. Earthquake Eng., Beijing, China, 8 pp.

Tehranizadeh M. and Hamedi F.; 2000: *Influence of effective duration of strong motion on elastic response spectra*. In: Proc. 12th World Conf. Earthquake Eng., Auckland, New Zealand, 7 pp.

Uthayakumar U.M. and Naesgaard E.; 2004: *Ground response analysis for seismic design in Fraser River Delta, British Columbia*. In: Proc. 13th World Conf. Earthquake Eng., Vancouver, Canada, 10 pp.

Wald D.J., Quintoriano V., Heaton T.H. and Kanamori H.; 1999: *Relationship between peak ground acceleration, peak ground velocity and modified Mercalli intensity in California*. Earthquake Spectra, **15**, 557-564.

Zhang Z. and Stewart R.R.; 2007: *Seismic attenuation and rock property analysis in a heavy oilfield: Ross Lake, Saskatchewan*. CREWES Res. Report, Univ. of Calgary, Canada, Vol. 19, 16 pp.

Corresponding author: Bambang Setiawan
Faculty of Engineering, Syiah Kuala University
Jl. Tgk. Syech Abdurrauf 7, Darussalam, Banda Aceh, 23111, Indonesia
Phone: +62 821 78501824; e-mail: bambang.setiawan@unsyiah.ac.id